



## Physiology

## *Nicotiana tabacum* actin-depolymerizing factor 2 is involved in actin-driven, auxin-dependent patterning

Steffen Durst, Peter Nick, Jan Maisch\*

Botanical Institute, Molecular Cell Biology, Karlsruhe Institute of Technology (KIT), Kaiserstraße 2, D-76131 Karlsruhe, Germany

## ARTICLE INFO

## Article history:

Received 8 January 2013  
 Received in revised form 7 March 2013  
 Accepted 7 March 2013  
 Available online 30 March 2013

## Keywords:

Actin  
 Actin-binding proteins  
 Auxin signalling  
 Cell division pattern  
 Tobacco BY-2

## ABSTRACT

Polar transport of auxin has been identified as a central element of pattern formation. To address the underlying cellular mechanisms, we use the tobacco cell line (*Nicotiana tabacum* L. cv. Bright Yellow 2; BY-2) as model. We showed previously that cell divisions within a cell file are synchronized by polar auxin flow, linked to the organization of actin filaments (AF) which, in turn, is modified via actin-binding proteins (ABPs). From a preparatory study for disturbed division synchrony in cell lines overexpressing different ABPs, we identified the actin depolymerizing factor 2 (ADF2). A cell line overexpressing GFP-NtADF2 was specifically affected in division synchrony. The cell division pattern could be rescued by addition of Phosphatidylinositol 4,5-bisphosphate (PIP<sub>2</sub>) or by phalloidin. These observations allow to draw first conclusions on the pathway linking auxin signalling via actin reorganization to synchronized cell division placing the regulation of cortical actin turnover by ADF2 into the focus.

© 2013 Elsevier GmbH. All rights reserved.

## Introduction

Auxin plays a key role in the transmission of environmental and endogenous signals. Originally defined as enhancer of cell elongation (Normanly et al., 2010), auxin regulates, in addition, apical dominance, leaf senescence, fruit setting, growth and ripening, and plays an essential role in tropistic responses to light and gravity (for review see Davies, 2010). As a central function, auxin defines directional cues fundamental to patterning (for review see Berleth and Sachs, 2001). These patterning events depend, in many cases, on a directional flow of auxin. This cell-to-cell process has been described by a modified chemiosmotic model (for review see Lomax et al., 1995), implying influx through locally confined carriers and an (ubiquitously active) ion-trap mechanism, and locally confined efflux through different carriers. Auxin-dependent patterning phenomena, such as the transdifferentiation of parenchymatic cells into vasculature (for review see Sachs, 2000), or the definition of new primordia in phyllotaxis (Reinhard et al., 2000) therefore depend on cell polarity. Cell polarity and polar auxin flow are linked by dynamic localization of the efflux carriers through directional intracellular traffic in a self-

amplifying feedback loop. Directional flux through carriers and non-directional influx by the ion trap generates a lateral inhibition, resulting in an ordered pattern (for review see Friml, 2010; Nick, 2010).

For patterning to occur, the directional efflux must adapt to local gradients of auxin. This adaptation seems to be brought about by cycling of transporters (Dhonukshe et al., 2008). This cycling is modulated by actin organization. When actin assembly is inhibited, this affects the polar localization of several transporters including PIN1, PIN3, and the auxin-influx carrier AUX1 (Kleine-Vehn et al., 2006; for review see Friml, 2010; Nick, 2010). Actin organization, in turn, is controlled by auxin. A fine, cortical network of dynamic actin is observed in cells that undergo auxin-triggered growth (Waller et al., 2002), whereas depletion of auxin is followed by the formation of stable actin bundles. The auxin-triggered reorganization of actin could later be confirmed *in vivo* (Holweg et al., 2004) and was shown to stimulate polar auxin transport (Nick et al., 2009) leading to an oscillator model where auxin signalling triggered the reorganization of F-actin bundles into finer filaments that, in turn, more efficiently transport auxin-signalling components towards the cell pole (for review see Nick, 2010).

To study the functional link between auxin and actin on the cellular level, we have established tobacco cell lines (such as BY-2 or VBI-0) as cellular model for simple auxin-dependent patterning. In these cell lines, the addition of auxin triggers a series of axial cell divisions generating a pluricellular cell file. The cell divisions within a cell file are partially synchronized. This partial synchrony leads to a pattern with elevated frequencies of files composed of an even number of cells (Campanoni et al., 2003; Maisch and Nick, 2007). The degree of division synchrony can be quantified

**Abbreviations:** ABP, actin-binding protein; ADF2, actin-depolymerizing factor 2; AF, actin filaments; BY-2, *Nicotiana tabacum* L. cv. Bright Yellow 2 suspension cell line; MI, mitotic index; NPA, 1-N-naphthylphthalamic acid; NtADF2 ox, BY-2 cell line overexpressing GFP-NtADF2; Lat B, latrunculin B; PIP<sub>2</sub>, Phosphatidylinositol 4,5-bisphosphate; WT, non-transformed BY-2 wild-type culture.

\* Corresponding author. Tel.: +49 721 608 42993; fax: +49 721 608 44193.

E-mail address: [Jan.Maisch@kit.edu](mailto:Jan.Maisch@kit.edu) (J. Maisch).

as frequency of even-numbered files. This type of division pattern had been shown to result from weak coupling between the divisions of neighbouring cells. Specifically, a diagnostic frequency peak of hexacellular files is indicative of synchronization of divisions by a signal transported unidirectionally through the cell file (Campanoni et al., 2003). This signal can be blocked by low concentrations of the auxin-transport inhibitor 1-N-naphthylphthalamic acid (NPA) that leave division activity and cellular morphology intact. Thus, division synchrony can be used to monitor polar auxin transport within the individual cell files. When actin was constitutively bundled by overexpression of YFP-mTalin, this synchrony was impaired. However, by exogenous auxins, a normal array of actin filaments (AF) could be restored and this rescued division synchrony (Maisch and Nick, 2007) demonstrating that a normal (debundled) configuration of actin was necessary and sufficient for the synchronization of cell division. It should be emphasized that this role of actin is merely regulatory and does not imply a function of actin in cell division itself. The impact of actin organization on division synchrony was interpreted in a model, where actin controls polar auxin transport through the file. The control of polar auxin transport by actin organization was subsequently demonstrated directly using transgenic rice plants overexpressing YFP-mTalin leading to excessive bundling of actin and reduced auxin flow measured directly using radioactively labelled indole acetic acid (Nick et al., 2009). Similar to the tobacco cell system, exogenous auxin could restore dynamic fine cortical AF and polar auxin flow.

The model of the actin–auxin oscillator postulates that the auxin signal must be conveyed to actin causing its reorganization. Neither the mechanism nor the players for this signalling have been identified. Since AFs can be modified by a plethora of actin-binding proteins (ABPs; for review see Staiger et al., 2010), it is likely that also the auxin signal could be mediated by one or a complex of several ABPs. To get better insight into the role of ABPs with regard to auxin-mediated actin-reorganization, we cloned besides the Lifeact peptide and the *Arabidopsis thaliana* fimbrin actin-binding domain 2 (Maisch et al., 2009) also selected members of different *Nicotiana tabacum* ABP families (actin-depolymerizing factor 2 (ADF2); Villin 1; WLIM-domain containing protein 2, WLIM2). We overexpressed them in tobacco BY-2 cells and probed the transgenic lines for alterations in division synchrony, mitotic index (MI), and cell elongation. From the results of this preliminary phenotyping tobacco ADF2 emerged as most promising candidate (Chen et al., 2002), since especially the division pattern of this transgenic line showed distinctive differences compared to the other ABP ox lines (such as Lifeact, AtFABD2, NtWLIM2, and NtVillin1) and the non-transformed BY-2 cell line.

ADFs bind to G- and F-actin with a noticeable preference for ADP-G-actin (Carrier et al., 1997; Blanchoin and Pollard, 1999). They disassemble AFs by a complex mechanism, which depends on the activity of stabilizing ABPs (Ketelaar et al., 2004; Huang et al., 2005). The activity of ADFs can be modulated by several factors, such as pH (Gungabissoon et al., 2001; Allwood et al., 2002), or phosphorylation of a N-terminal serine residue, which leads to a loss of actin-binding when phosphorylated (Allwood et al., 2001). In addition, the phosphoinositide lipid Phosphatidylinositol 4,5-bisphosphate (PIP<sub>2</sub>) can specifically inhibit actin-binding ability of ADFs (for review see Staiger et al., 2010).

In the present work we investigate the role of NtADF2 for auxin-dependent, patterned cell division in the homologous system. We report the cellular phenotype of a BY-2 cell line overexpressing GFP-NtADF2 (NtADF2 ox), analyzed its phenotype, and rescued the cell division pattern chemically with PIP<sub>2</sub> and phalloidin. These observations allow to draw first conclusions on the putative pathway from auxin signalling via actin reorganization and especially to role of actin stability for synchronized cell division in BY-2.

## Materials and methods

### Tobacco cell cultures

BY-2 (*Nicotiana tabacum* L. cv Bright Yellow 2) suspension cell lines (Nagata et al., 1992) were cultivated in liquid medium containing 4.3 g L<sup>-1</sup> Murashige and Skoog salts (Duchefa, <http://www.duchefa.com>), 30 g L<sup>-1</sup> sucrose, 200 mg L<sup>-1</sup> KH<sub>2</sub>PO<sub>4</sub>, 100 mg L<sup>-1</sup> inositol, 1 mg L<sup>-1</sup> thiamine, and 0.2 mg L<sup>-1</sup> (0.9 μM) 2,4-D, pH 5.8. The cells were subcultivated weekly, inoculating 1.0–1.5 mL of stationary cells into fresh medium (30 mL) in 100-mL Erlenmeyer flasks. The cells were incubated at 26 °C under constant shaking on a KS260 basic orbital shaker (IKA Labortechnik, <http://www.ika.de>) at 150 rpm. Every three weeks the stock BY-2 calli were subcultured on media solidified with 0.8% (w/v) agar (Roth, <http://www.carlroth.com>). Transgenic NtADF2 ox cells and calli were cultivated on the same media as non-transformed wild-type cultures (BY-2 WT), but supplemented with 25 mg L<sup>-1</sup> kanamycin.

### Generation of GFP-ADF2 construct

2 mL of cycling BY-2 WT (3 d after subcultivation, 100 mg of cells) were pipetted onto filter paper to remove the liquid medium. The cells were transferred with a spatula into a 2 mL reaction tube, immediately frozen in liquid nitrogen, and ground with a 5 mm steel bead in a TissueLyser (Qiagen, <http://www.qiagen.com>). Total RNA was extracted using a RNeasy Plant Mini Kit (Qiagen). Optional on-column digestion of genomic DNA was performed with RNase-free DNase I (Qiagen) according to the manufacturer instruction. Purity and integrity of the RNA-preparation were checked by electrophoresis. For reverse transcription, the Dynamo cDNA Synthesis Kit (Finnzymes, <http://www.finnzymes.com>) was used with 1 μg of RNA as template.

Plasmids for stable and transient transformation of BY-2 WT cells were constructed via Gateway®-Cloning (Invitrogen, <http://www.invitrogen.com>). The sequence encoding the *N. tabacum* ADF2 (Chen et al., 2002) was amplified by PCR using oligonucleotide primers (Supplementary Data S1). The size of the amplicon was verified by electrophoresis and purified via NucleoSpin® Extract II (Machery-Nagel, <http://www.mn-net.com>) according to the manufacturer instructions. The resulting full length cDNA of NtADF2 was inserted into the binary vector pK7WGF2 (Karimi et al., 2002) containing a CaMV 35S promoter and a N-terminal GFP as fluorescent marker. The sequence of the fusion construct was verified by restriction digest and sequencing (GATC, <http://www.gatc-biotech.com>).

### Transient and stable transformation of tobacco BY-2 cells

Biolistic transformation was performed as described in Maisch et al. (2009). Following bombardment, the cells were incubated for 4–24 h in the dark at 26 °C, and observed under the fluorescence microscope.

Stable transformation of BY-2 cells with the binary vector construct pK7WGF2-NtADF2 was achieved according to An (1985) with minor modifications as described in Maisch et al. (2009). Cell-suspension cultures were established from calli using 25 mg L<sup>-1</sup> kanamycin added to the liquid medium for selection.

### Determination of NtADF2-expression by semi-quantitative RT-PCR

The overexpression of the introduced NtADF2 in the NtADF2 ox cell line was verified by semi-quantitative RT-PCR in samples from non-transformed BY-2 WT and NtADF2 ox cells collected at day 4 after subcultivation. The reverse transcription, performed as

described above, was followed by a PCR using standard Taq polymerase (NEB, <http://www.neb.com>) according to the manufacturer instructions. For detection of NtADF2 cDNA levels in tobacco BY-2, the primers sqNtADF2\_fw 5'-AGT GCC GCT ATG CTG TCT TTG-3' and sqNtADF2\_rv 5'-GTG TCA GGT GAC CAA GCA ATG-3' were used. NtActin (sqNtActin\_fw 5'-ACA ACG AGC TTC GTG TTG C-3' and sqNtActin\_rv 5'-CAG TGT GAC TCA CAC CAT CAC-3') and NtGAPD (Hu et al., 2010) were used as internal standards (Supplementary Data S2). The gels were quantified by grey-value analysis in ImageJ (NIH, <http://rsbweb.nih.gov/ij>).

#### Visualization of actin filaments (AF)

AFs were visualized by the method of Kakimoto and Shibaoka (1987) modified according to Olyslaegers and Verbelen (1998) as described in Maisch et al. (2009).

#### Phenotyping of BY-2 lines

Division synchrony of tobacco BY-2 cells was quantified by collecting 0.5-mL aliquots of cells 4 d after subcultivation and immediate observation under an AxioImager Z.1 microscope (Zeiss, <http://www.zeiss.de>). Differential interference contrast images were obtained by a digital imaging system (AxioVision; Zeiss). For each picture, the MosaiX module of the AxioVision software was used to cover a 5 mm × 5 mm area. Using the stitching-function, frequency distributions over the number of cells per individual file were constructed (Maisch and Nick, 2007). Each data point represents between 921 and 1158 cell files from three independent experimental series. The differences between control cell line and transgenic/treated cell line of each data point were tested for significance by a *t*-test at the 95% confidence level.

The mitotic index (MI) of tobacco BY-2 cell suspension was determined following fixation with Carnoy fixative and nuclear dye Höchst 33258 (2'-(4-hydroxyphenyl)5-(4-methyl-1-piperazinyl)-2,5'-bi(1H-benzimidazole)-trihydrochloride; Sigma–Aldrich, <http://www.sigmaaldrich.com>), as described in Maisch and Nick (2007). Samples were observed under an AxioImager Z.1 microscope (Zeiss) using the filter set 49 (excitation at 365 nm, beamsplitter at 395 nm, and emission at 445 nm). MIs were determined as the relative frequency of mitotic cells out of a sample of 500 cells scored for each data point.

Cell length and width were determined from the central section of the cells using the length function of the AxioVision software according to Maisch and Nick (2007). Each data point represents average and standard error from 500 individual cells from three independent experimental series. Division synchrony, MI, cell length and width were observed to be not affected by kanamycin selection.

#### Microscopy and image analysis

For morphological studies, cells were examined under an AxioImager Z.1 microscope (Zeiss) equipped with an ApoTome microscope slider for optical sectioning and a cooled digital CCD camera (AxioCam MRm; Zeiss). TRITC- and GFP-fluorescence were observed through the filter sets 43 HE (excitation: 550 nm, beamsplitter: 570 nm, emission: 605 nm) and 38 HE (excitation: 470 nm, beamsplitter: 495 nm, emission: 525 nm), respectively (Zeiss). Stacks of optical sections were acquired at different step sizes between 0.4 and 0.8  $\mu\text{m}$ .

For analysis of division pattern, cells were observed under the same microscope with a 20 $\times$  objective and differential interference contrast illumination. Images were processed for publication with respect to contrast and brightness using ImageJ (NIH).

#### Phosphatidylinositol 4,5-bisphosphate (PIP<sub>2</sub>), phalloidin, latrunculin B (Lat B) and auxin treatments

PIP<sub>2</sub> (Sigma–Aldrich) was added at inoculation from filter-sterilized stocks of 2 mM in chloroform:methanol:0.5 M HCl (10:5:1, by vol.) to a final concentration of 50 nM, a concentration that had been found in preparatory studies to leave cell division and culture growth unaffected.

Phalloidin from *Amanita phalloides* (Sigma–Aldrich) was added directly to the final concentration of 1  $\mu\text{M}$  into the standard culture medium using a filter-sterilized stock of 1 mM phalloidin dissolved in 96% (v/v) ethanol.

Lat B from *Latrunculia magnifica* (Sigma–Aldrich) was added directly to the final concentration of 65 nM into the standard culture medium using a filter-sterilized stock of 1 mM Lat B dissolved in 96% (v/v) ethanol.

NPA (1-N-naphthylphthalamic acid, Sigma–Aldrich) was added at inoculation from a filter-sterilized stock of 10 mM in dimethyl sulfoxide to a final concentrations of 10  $\mu\text{M}$ . Auxins were also added directly to the final concentration of 2  $\mu\text{M}$  into the standard culture medium using filter-sterilized stocks of 10 mg mL<sup>-1</sup> IAA (Sigma–Aldrich) and 10 mg mL<sup>-1</sup> 2,4-D (Sigma–Aldrich) dissolved in 96% (v/v) ethanol, respectively.

Equal aliquots of sterile solvents were added to the control samples as solvent controls.

## Results

### NtADF2 – a member of ADF-subgroup 2

Tobacco ADF2 (AAL91667; Chen et al., 2002) was chosen as promising candidate for auxin-dependent actin reorganization from a preparatory study for altered division pattern where frequency distributions over the number of cells per individual file were investigated. As compared to lines overexpressing ABPs such as Lifeact or AtFABD2 and tobacco ABPs such as NtVillin1 or NtWLIM2, the overexpression of NtADF2 altered the division pattern massively (Supplementary Data S3). NtADF2 clusters together with NtADF1 into subgroup 2 of plant ADF/cofilin members (Maciver and Hussey, 2002), defined as group exclusively present in pollen (Fig. 1a).

NtADF2 is predicted to consist of 137 amino acid residues with a molecular mass of 15 kD (Chen et al., 2002) and several highly conserved domains. A serine-6 identified as phosphorylation site (Chen et al., 2002) is followed by an actin-binding motif (amino acids 6, 7, 96, 98, 123 and 126). This actin-binding motif is accompanied by a second signature specific for F-actin binding with conserved amino acids 80, 82, 134 and 135. Interestingly, from amino acid 22–28, a predicted nuclear localization sequence is highly conserved in NtADF2 as in all former investigated ADF homologs (Maciver and Hussey, 2002). Moreover, NtADF2 also contains all positively charged amino acids essential for the electrostatic interaction with PIP<sub>2</sub> (Zhao et al., 2010) at position 80 (K), 98 (K), 109 (K), 110 (R) suggesting that NtADF2 is able to interact with and can be regulated by PIP<sub>2</sub>.

### Intracellular localization of NtADF2

To get insight into the role of NtADF2 for actin organization and auxin-dependent patterning, we overexpressed a fusion between GFP and the *N. tabacum* ADF 2 (NtADF2) in the homologous system BY-2, either by transient transformation via particle bombardment (Fig. 2a–c) or in a stable manner via *Agrobacterium tumefaciens* followed by selection on kanamycin leading to the NtADF2 ox cell line (Fig. 2d–f).

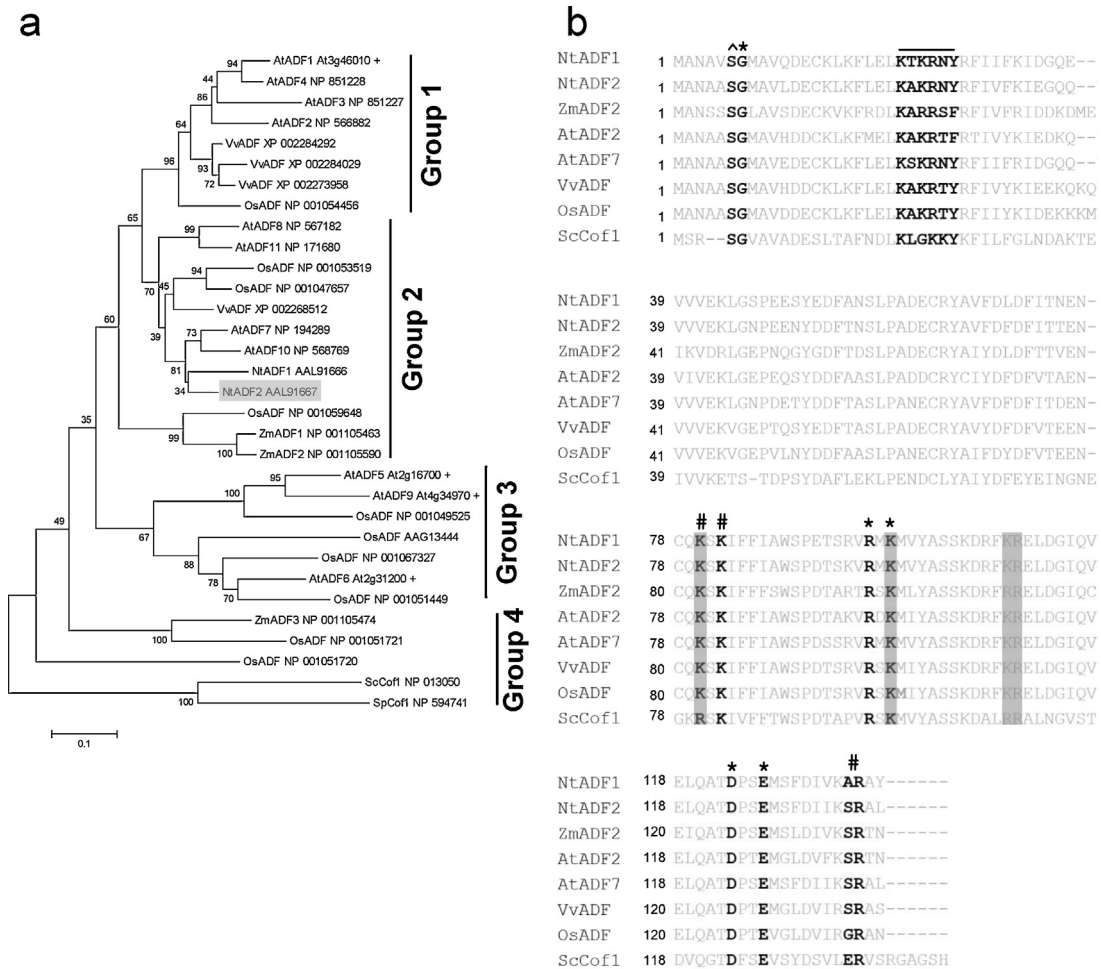


**Fig. 1.** (a) Phylogenetic tree of representative model plant ADFs. An alignment of the complete sequences was made with MEGA 4.1 (beta 3); from this data a phylogenetic tree was derived using neighbour-joining method and bootstrapping (1000 reiterations). The output tree was plotted also using MEGA 4.1 (beta 3). All data were taken from published literature and genomic databases. With a plus-marked entries are listed in Tree Families Database (Treefam; <http://www.treefam.org/>) of the Sanger Institute, all other entries are derived from the National Center for Biotechnology Information database (NCBI; <http://www.ncbi.nlm.nih.gov/>). Categorization into 4 groups was performed in accordance with Maciver and Hussey (2002). *Arabidopsis thaliana* AtADF; *Vitis vinifera* VvADF; *Oryza sativa* OsADF; *Zea mays* ZmADF; as outgroup coflin 1 of *Saccharomyces cerevisiae* ScCof1 and *Schizosaccharomyces pombe* SpCof1 were used. (b) Alignment of selected representative model plant ADFs derived from phylogenetic tree analysis of (a). As representative protein sequences of *Vitis vinifera* VvADF XP.002284292 and for *Oryza sativa* OsADF NP.001054456 were chosen. All other sequences correspond to (a). Black colour marks important protein domains: Phosphorylation site *circumflex*; G-actin-binding sites *asterisks*; nuclear localization site *underline*; specific F-actin-binding sites *number sign* (NCBI); PIP<sub>2</sub> interacting sites *grey boxes* (Zhao et al., 2010). For accession numbers see Supplementary Data S8.

Fig. 2a–c exemplarily shows transiently transformed BY-2 cells 4 h (a), 17 h (b), and 24 h (c) after biolistic transformation. To test for potential changes dependent on the development of the culture, we performed this experiment at different time points. As shown exemplarily for 3 d (b), 4 d (a), and 5 d (c) after subcultivation, GFP-NtADF2 labelled filamentous structures that resembled actin bundles consistent with observations in transformed pollen tubes (Chen et al., 2002). The fine cortical filaments visualized by other markers such as GFP-FABD2 (Maisch et al., 2009; Supplementary Data S4) were not observed. Additionally to the bundled filaments, the GFP-signal was found in the cytoplasm, independent of culture stage and incubation time after biolistic transformation. It should be mentioned that those cells that displayed bundled actin, also displayed symptoms indicative of ensuing cell death (data not shown). Cytoplasmic localization was also dominant in the stably transformed tobacco cell line ( $89.4 \pm 5.3\%$ , Fig. 2d). However, in a subpopulation of stably transformed cells, the GFP marked filamentous ( $4.7 \pm 0.8\%$ , Fig. 2e) or fragmented structures ( $5.9 \pm 1.2\%$ , Fig. 2f). Moreover, the GFP-signal was found in the interphase nucleus of stably transformed GFP-NtADF2 ox cells as well (Supplementary Data S5c).

To test, whether these filaments visualized by the GFP-marker are AFs, the NtADF2 ox line was stained with TRITC-phalloidin. Since phalloidin and ADF2 share their binding site on actin, they are expected to compete for binding (Nishida et al., 1987; Hayden et al., 1993; Jiang et al., 1997). In fact, in the staining experiment, most cells either showed the GFP-labelled bundles or the TRITC-labelled AFs. However, in a small subpopulation of cells, where the GFP-signal was moderate, dual visualization was successful (as exemplarily shown in Fig. 2h). Comparison of actin organization revealed some differences with respect to the existence of fine AFs. Whereas the actin cables in the transgenic line (Fig. 2j1) were comparable to those in non-transformed cells (Fig. 2i1), the fine cortical actin meshwork was either depleted (Fig. 2b) or highly fragmented (Fig. 2f and j2). This was in contrast to non-transformed BY-2 WT cells (Fig. 2i2). Interestingly, after pretreatment with unlabelled phalloidin for 3 d we were able to visualize more fine AFs in NtADF2 ox cells (Fig. 2j3), although non-transformed BY-2 WT cells were only minimally impaired by this treatment (Fig. 2i3).

To test, whether NtADF2 might, in addition to its function in regulating the synchrony of cell division, directly participate in

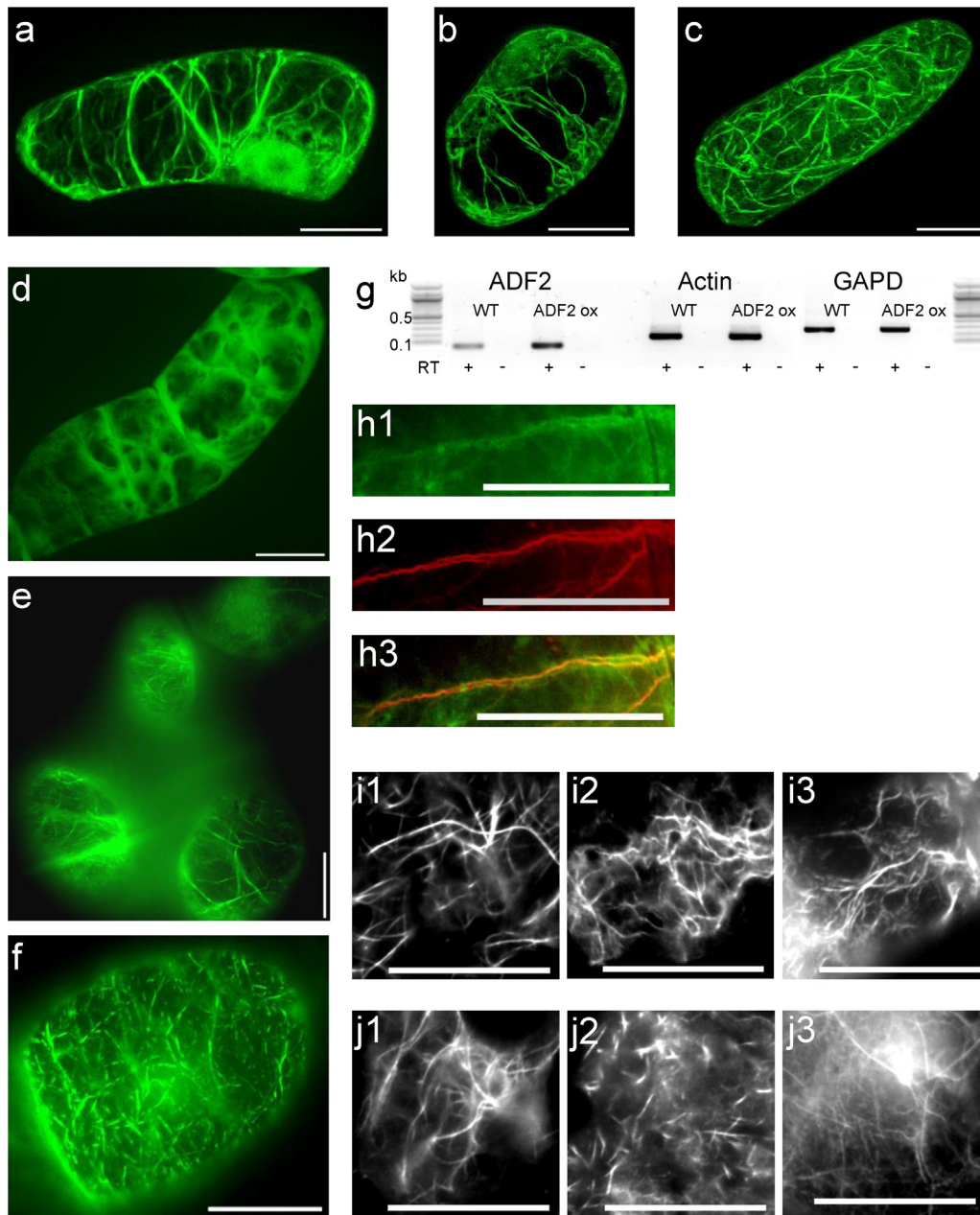


**Fig. 2.** Localization and expression of GFP-NtADF2 in GFP-NtADF2-transformed tobacco BY-2 cells. (a–c) Transient transformed BY-2 cells 4 h (a), 17 h (b) and 24 h (c) after biolistic transformation. Stable NtADF2 ox cells showed cytoplasmic localized GFP-signal (d) and filamentous (e) or fragmented structures (f). (g) Semi-quantitative PCR using *Nicotiana tabacum* actin and GAPD as reference genes. Lines marked with *minus* are samples prepared without reverse transcriptase. (h) Exemplarily shown multi channel confocal images and details of TRITC-phalloidin-stained cells: GFP-ADF2 (1); TRITC-phalloidin (2); Merge (3). (i) Details of TRITC-phalloidin-stained non-transformed BY-2 cells as reference for bundled (1), fine (2) and phalloidin-pretreated AFs (3). (j) Details of TRITC-phalloidin-stained NtADF2 ox cells showing bundled (1), fine (2) and phalloidin-pretreated AFs (3). Bars = 20  $\mu$ m.

cell division itself, we followed the localization of GFP-NtADF2 through the different phases of mitosis and cell division (Supplementary Data S5). However, we observe that the GFP signal was spread throughout the cytoplasm and unspecifically followed the dynamic changes of cytoplasmic strands accompanying mitosis and cell division. From this localization pattern no specific function for cell division itself can be inferred.

To verify the expression of the transgene, we performed a semi-quantitative PCR using cDNA prepared at 4 d after subcultivation. Fig. 2g shows an elevation of GFP-NtADF2 transcript level in the NtADF2 ox cell line over the non-transformed BY-2 WT by a factor of about 3. As reference genes, *N. tabacum* actin and Glyceraldehyde 3-phosphate dehydrogenase (GAPD) were used.

#### *NtADF2*-overexpression alters MI and cell elongation

To identify possible effects of NtADF2-overexpression on cell morphology a phenotypic analysis was performed. We followed MI, cell length, and cell width of the NtADF2 ox cell line compared to the non-transformed BY-2 WT control through the entire culture cycle. As shown in Fig. 3a, MI was diminished in the NtADF2 ox cell line by 20–30% in comparison to the control from day 1 after subcultivation.

Parallel to the MI, the ratio of cell length and cell width was followed as measure for proportionality, as the cells of the NtADF2 ox appeared more stunted than the non-transformed control. Since BY-2 WT and NtADF2 ox did not differ in width ( $34.6 \pm 1.8 \mu$ m)

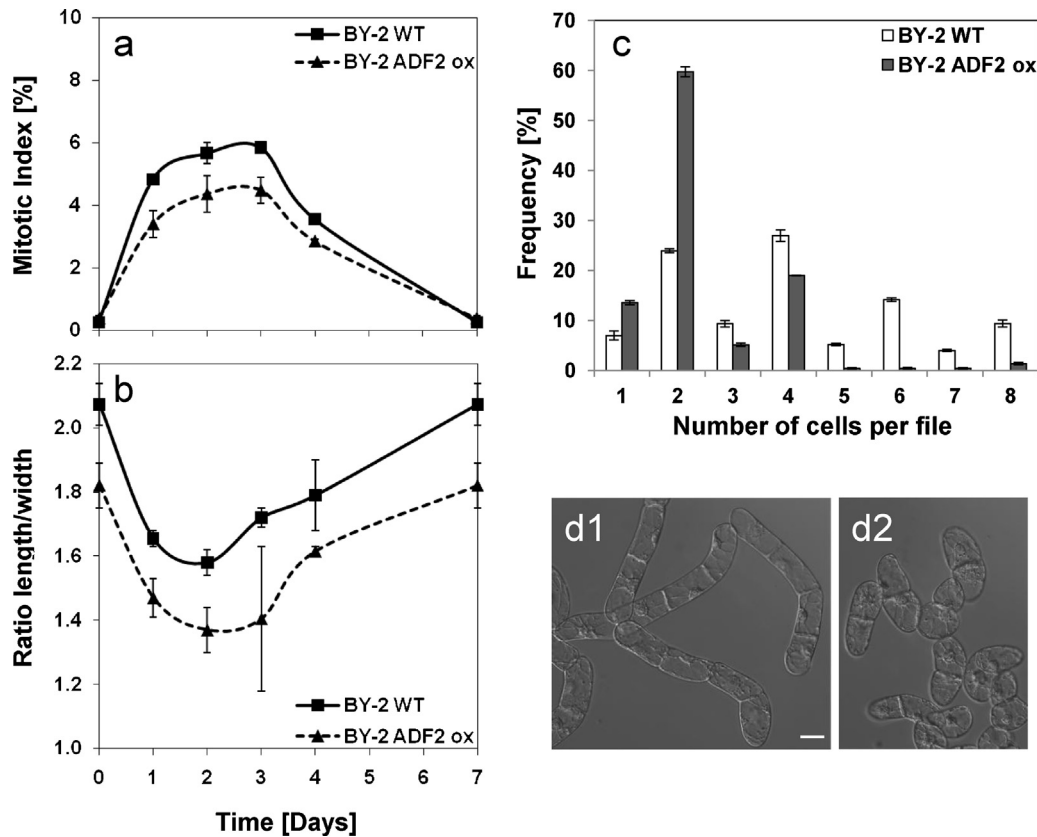


**Fig. 3.** Phenotypic analysis of BY-2 WT (filled boxes, continuous curve) and NtADF2 ox (filled triangles, dashed curve) tobacco cell cultures. (a) MI (mean of  $n = 1500$ ). (b) Cell elongation as ratio of cell length over cell width (mean of  $n \geq 1000$ ). (c) Division pattern 4 d after subcultivation of BY-2 WT (white bars) and NtADF2 ox (black bars) tobacco cell cultures (mean of  $n = 921$ – $1158$ ). All experimental data are derived from three independent experimental series; error bars = SE. (d) Representative cell files of BY-2 WT (d1) and NtADF2 ox (d2) 4 d after subcultivation. Bar =  $20 \mu\text{m}$ .

throughout the whole cultivation cycle, the impression was exclusively caused by a reduced cell length in the NtADF2 ox line ( $13 \pm 3\%$ , Fig. 3b).

#### NtADF2-overexpression alters division patterns in BY-2 cells

Divisions are synchronized by a polar flow of auxin over a cell file (Campanoni et al., 2003), and this pattern is highly sensitive to perturbations of actin (Maisch and Nick, 2007). We therefore monitored cell-division patterns in the NtADF2 ox cell line in comparison with non-transformed controls. In fact, the pattern was altered in the NtADF2 ox as monitored by frequency distributions over the number of cells within individual files. The non-transformed BY-2 cells showed a characteristic oscillatory behaviour with clear peaks at even cell numbers (Fig. 3c). In particular, a clear peak at 6 cells per file indicating directional auxin-dependent synchrony (Campanoni et al., 2003) could be observed. In contrast, this pattern was affected in the NtADF2 ox. Here, bicellular files were 2.5-fold more common, whereas the frequency of quadricellular files was reduced by almost 30%. Files with a larger number of cells were almost completely missing (Fig. 3c), such that the average number of cells per file dropped to 2.43 (as compared to 4.05 in the non-transformed BY-2 WT cell line). Representative cell files are shown in Fig. 3d. The difference between the lines was persistent when the selective pressure on the cell line was removed by omitting kanamycin from the medium (data not shown), confirming that the disturbed pattern was an effect of the transgene and not an effect of the selection pressure.

#### Disturbed morphology and division pattern in the NtADF2 ox can be partially rescued by PIP<sub>2</sub> and phalloidin

As NtADF2 contains a PIP<sub>2</sub> interaction site, and PIP<sub>2</sub> is able to compete with actin for ADF-binding, we tested, whether the phenotype of the NtADF2 ox could be rescued by addition of exogenous PIP<sub>2</sub>.

PIP<sub>2</sub> was diluted from a 2 mM stock solution to a final concentration of 50 nM in the standard cultivation medium. As control, every experiment was conducted with the same volume of the solvent. These solvent controls showed no detectable effects (data not shown). As illustrated in Fig. 4a1, we were able to completely rescue the diminished MI of the NtADF2 ox cell line. Tests for potential negative effects on cell viability did not reveal any significant difference between treated and untreated cells (data not shown).

With regard to division pattern, assessed at the end of the logarithmic phase, 4 d after subcultivation and addition of PIP<sub>2</sub> to the NtADF2 ox, we were able to observe a partial rescue. The strong frequency peak for bicellular files was clearly reduced by  $22.0 \pm 2.8\%$  in the treated cell culture. The reduced frequency peak for quadricellular files was completely rescued by 50 nM PIP<sub>2</sub> to the level observed in non-transformed BY-2 WT cells. Most interestingly, the peak at 6 cells per file, indicating polar auxin transport (Campanoni et al., 2003) and completely eliminated as consequence of ADF2-overexpression, was partially restored (Fig. 4a2) as well as the peak for files composed of 8 cells (frequencies of  $5.2 \pm 1.1$  and  $4.4 \pm 0.7$ ). The division pattern of non-transformed BY-2 WT cells remained largely unaltered (Supplementary Data S6).

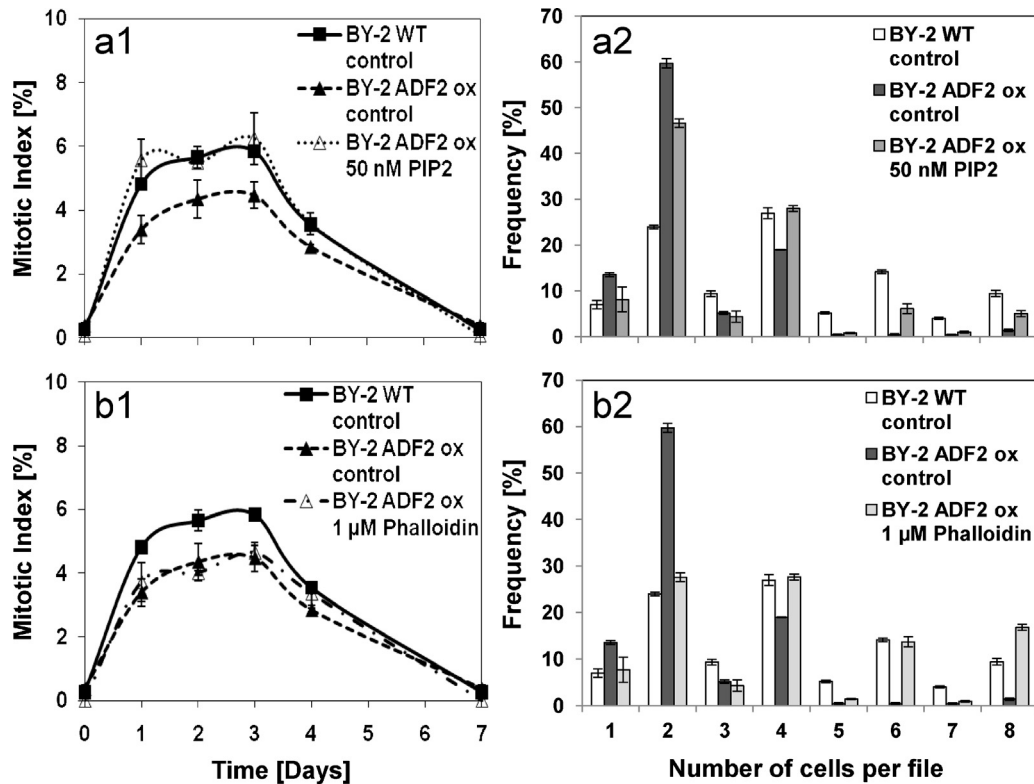


**Fig. 4.** Effect of PIP<sub>2</sub> (a) and phalloidin (b) on MI and division pattern. BY-2 WT control (filled boxes, continuous curve and white bars, respectively), NtADF2 ox control (filled triangles, dashed curve and black bars, respectively), NtADF2 ox PIP<sub>2</sub>-treated (open triangles, dotted line and grey bars, respectively) and NtADF2 ox phalloidin-treated (open triangles, dash-dotted curve and light grey bars, respectively) tobacco cell cultures.

In a second approach we treated the NtADF2 ox and the non-transformed BY-2 WT lines with phalloidin at a working concentration of 1  $\mu$ M, a concentration that in BY-2 causes a mild stabilization of actin without causing toxicity (Berghöfer et al., 2009). For the reduced MI of the NtADF2 ox that had been completely rescued by PIP<sub>2</sub>-treatment, no effect was detectable. MI remained diminished by 20–30% throughout the cultivation cycle as compared to the non-transformed BY-2 WT (Fig. 4b1).

When the division pattern was scored at the end of the logarithmic phase, 4 d after subcultivation, there was no significant effect of phalloidin on the non-transformed BY-2 WT except the slight tendency to cell files with a larger number of cells observed in both cell lines. The characteristic pattern with elevated frequencies of even-numbered cell files was maintained (Supplementary Data S6). In contrast, the aberrant division pattern of the NtADF2 ox was rescued by phalloidin and now was nearly identical to the BY-2 WT pattern. The massive peak at two cells per file was reduced to that of the non-transformed BY-2 WT (Fig. 4b2). Conversely, the effect of 65 nM Lat B in the non-transformed BY-2 WT line was comparable to the affected division pattern of the untreated NtADF2 ox line (Supplementary Data S7).

We further investigated how the pattern of cell division responded to manipulation of auxin transport. Neither treatment with auxins (2  $\mu$ M IAA, 2  $\mu$ M 2,4-D) nor with NPA (10  $\mu$ M NPA), an inhibitor of polar auxin transport, altered the disturbed division pattern of the NtADF2 ox line significantly (Supplementary Data S7).

## Discussion

In this work we analyzed localization and potential function of NtADF2, a member of the ADF/cofilin-family. We created, to our knowledge, the first stable NtADF2 ox BY-2 cell line, which gave

us the opportunity to visualize intracellular localization of NtADF2 *in vivo*. We were able to identify a possible ADF2 function for the stability of fine AFs and auxin-dependent division patterning in BY-2 cell files. By means of a NtADF2 ox cell line, we were able to study ADF functions in the homologous system and to rescue the altered cell division pattern of this cell line chemically with PIP<sub>2</sub> and phalloidin. In particular, we could restore the frequency peak for hexacellular files diagnostic for functional division synchrony (Campanoni et al., 2003). Although our data suggest a role of ADF2 for the synchrony of cell divisions, we do not have any indication that ADF2 participates in the process of cell division itself. For instance, during mitosis and cytokinesis, the GFP-NtADF2 fusion is spread in a diffuse manner throughout the cytoplasm and is not associated with any of the specific actin arrays observed during cell division.

Phylogenetic analysis using representative plant homologues of selected model plants revealed that NtADF2 contains all characteristic domains of the ADF/cofilin family including a PIP<sub>2</sub> interaction side and clusters together with NtADF1 into subclass II of the plant ADF2 phylogenetic tree (see Fig. 1b) described by Mun et al. (2000) and extended by Maciver and Hussey (2002). This subclass II is defined as “pollen exclusive expressed”. Since the isolation of two “pollen-specific” paralogs of ADFs (Chen et al., 2002), no additional ADFs had been reported for *N. tabacum*. This is quite untypical for plants which normally possess more ADFs than animals (Maciver and Hussey, 2002). Since we cloned NtADF2 from a non-transformed BY-2 line, it must be at least transcribed in BY-2 cells (see Fig. 2g) even though they propagate vegetatively.

Plant actin is organized in several morphologically and probably functional different subpopulations. Most prominent are the fairly stable transvacuolar cables that interconnect to a dynamic actin meshwork in the cell cortex and are linked to membrane stability (Hohenberger et al., 2011). It seems that this cortical actin

network is the main target of ADF2: Upon transient overexpression of GFP-NtADF2, the cortical actin meshwork was totally absent or fragmented (Fig. 2j2). In contrast, thick transvacuolar actin cables could be detected (Fig. 2a–c and j1). This shift towards the bundled conformation is expected when ADF preferentially acts on the more dynamic cortical AFs. ADF binds at the pointed-end and twists the filament leading to an enhanced decay (for review see Bamberg et al., 1999). In contrast, actin cables that are stabilized by actin-bundling proteins, persist. In fact, when AFs are bundled by overexpression of mouse-talin (Ketelaar et al., 2004) or *Arabidopsis*-villin (Huang et al., 2005) escape the depolymerizing activity of ADF *in vitro*. The thick AFs observed after transient transformation in some cells, probably persisted because they were protected from depolymerization due to their bundling. Since these cells were obviously stressed, these actin bundles might be the manifestation of ensuing cell death (for review see Smertenko and Franklin-Tong, 2011). Thus, these bundles are not produced by ADF2, but are observed, because they persist to ADF2.

Beside this bundled filamentous localization a strong cytoplasmic and nuclear GFP-signal was detectable (see Fig. 2a and d), probably due to the high affinity of ADFs for G-actin (Carrier et al., 1997; Blanchoin and Pollard, 1999). To test for potential effects of overexpression or cell cycle we checked different incubation times and cell ages, but did not detect any significant effects on localization (see Fig. 2a–c). The absence of fine filaments was confirmed by the observation of the stable transformant (see Fig. 2d–f), and is congruent with findings published for pollen tubes (Chen et al., 2002). The GFP-signal was also found in the interphase nucleus of stably transformed GFP-NtADF2 ox cells, but not in GFP-NtVillin 1 ox cells (Supplementary Data S3b). Due to the low molecular mass of ADFs and their small size underneath the size exclusion limit of the nuclear pores, they are most likely able to enter the nucleus also in their GFP-tagged state in contrast to the large ABPs of the Villin family.

The phenotypic characterization revealed clear differences between non-transformed and NtADF2 ox cell culture. NtADF2 ox cells were significantly shorter and exhibited a reduced MI (see Fig. 3a and b), indicating that, due to the overexpression of NtADF2, there are less fine filaments left or stable enough to fulfil their role in intracellular trafficking, affecting growth and the progression through interphase. Similar results have been shown by Chen et al. (2002) for tip growth in tobacco pollen tubes and by Dong et al. (2001) for longitudinal growth of *A. thaliana* cotyledons, hypocotyls and roots at the seedling stage.

Non-transformed BY-2 cells grow in files up to eight cells per file with an enhanced amount of even-numbered cells per file before decay into shorter even-numbered files. This synchronized file growth is dependent on polar auxin flow (Maisch and Nick, 2007; Nick et al., 2009; for review see Nick, 2010). The NtADF2 ox cell line behaved significantly different. Files with more than four cells were hardly detectable (see Fig. 3c). Thus, the depolymerization of fine AFs, caused by overexpression of NtADF2, interfered with the auxin-dependent synchrony of cell division. This synchrony should be, at least partially, restored when fine AFs are protected from depolymerization via exogenous PIP<sub>2</sub> which competes with F-actin binding of NtADF2 reducing the depolymerizing activity of NtADF2. In fact, we were able to partially restore the division pattern by exogenous PIP<sub>2</sub> (see Fig. 4a2) indicating the participation of NtADF2.

In the next experiment we asked, whether a rescue can be achieved by reducing actin dynamics per se. If the missing existence of stable fine filaments is the reason for the impaired division synchrony, the stabilization of the fine AF should decrease ADF depolymerizing activity and rescue the normal division pattern in the NtADF2 ox line as well. To test this reasoning, we treated the NtADF2 ox cell line with phalloidin. Indeed, the phalloidin

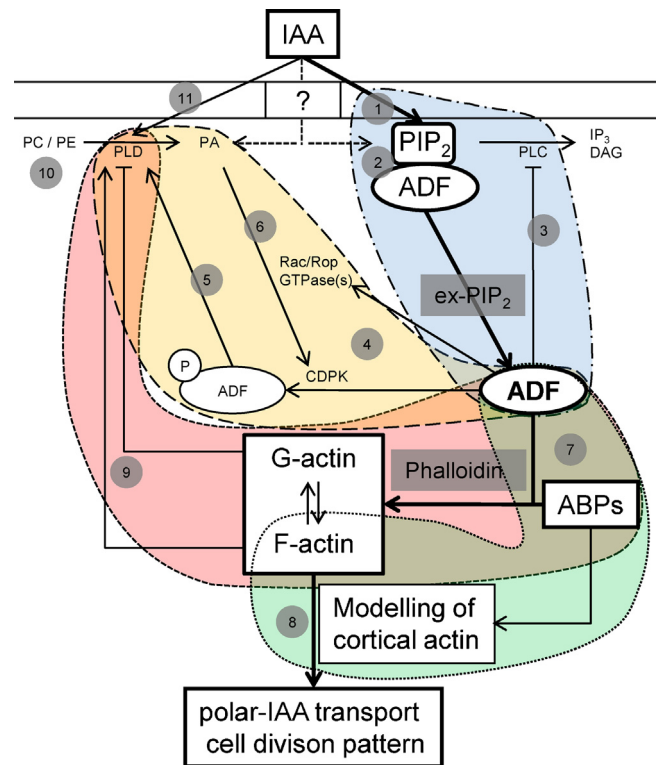


**Fig. 5.** Model of the putative pathway from auxin signalling via actin reorganization to synchronized cell division (arrows in bold; regulatory mechanisms: I cyan, II yellow, III red, IV green). For further details, see section "Discussion". References: (1) Lanteri et al. (2008); (2) Van Troys et al. (2008); (3) Gungabissoon et al. (1998); (4) Chen et al. (2003); (5) Bernstein and Bamberg (2010); (6) Farmer and Choi (1999); (7) Bernstein and Bamberg (2010); Staiger et al. (2010); (8) Maisch and Nick (2007), Nick et al. (2009); (9) Pleskot et al. (2010); (10) Wang (2000); (11) Lanteri et al. (2008).

treatment resulted in a complete rescue of division pattern in the NtADF2 ox cell line (see Fig. 4b2) at a concentration that did not cause a significant effect on the non-transformed control culture (see Supplementary Data S6). This supports our suggestion that the stability of F-actin plays a pivotal role in auxin-dependent patterning. These results are supported by phenotypic characterizations of additional actin marker lines overexpressing actin-bundling proteins like NtVillin1 or NtWLM2 (data not shown), and Lat B treatment of non-transformed BY-2 WT cells (see Supplementary Data S7), respectively.

Our observations can be integrated into a first working model comprising a putative pathway from auxin signalling via actin reorganization to synchronized cell division. Our working model highlights on four interdigitated regulatory mechanisms:

- (i) (Fig. 5, cyan) Auxin passes the cell membrane via diffusion or transmembrane proteins (Laňková et al., 2010) activating several auxin-dependent pathways, among others, ADF-related events. Here, one of the first steps is the alteration of the PIP<sub>2</sub> level in the inner membrane layer causing a rapid and transient accumulation of PIP<sub>2</sub> (Lanteri et al., 2008). Subsequently, more PIP<sub>2</sub> interacts with ADF, hindering its actin binding site. This leads to a reduced depolymerization activity of ADF. Additional to this interaction, ADF is able to inhibit the activity of PLC (Gungabissoon et al., 1998), thus raising the PIP<sub>2</sub> level even further.
- (ii) (Fig. 5, yellow) A second regulatory mechanism is based on the phosphorylation state of ADF. This phosphorylation at serine-6 is mediated by a yet unidentified Ca<sup>2+</sup>-dependent kinase (CDPK), which, in turn, is affected by Rac/Rop GTPases

(Smertenko et al., 1998; Allwood et al., 2001; Chen et al., 2003). Phosphorylated ADF is not able to depolymerize actin and was long thought to be a completely inactive form of the protein. However, Han et al. (2007) could show a direct stimulation of PLD activity for phosphorylated ADF/cofilin which is again linked to a CDPK via phosphatidic acid (PA) signalling (Farmer and Choi, 1999).

- (iii) (Fig. 5, red) In interaction with other ABPs like profilin, capping proteins (for review see Staiger et al., 2010), or actin-related proteins (for review see Bernstein and Bamberg, 2010), ADF affects actin dynamics and conformation by modulation of the equilibrium between polymerized F-actin and cytoplasmic G-actin. Both forms of actin are able to interact directly with PLD to control their intracellular amount. G-actin inhibits PLD-activity, whereas F-actin is stimulating (Pleskot et al., 2010), such that ADF-phosphorylation rate can be regulated via this pathway (see regulatory mechanism II).
- (iv) (Fig. 5, green) Downstream of the three described regulatory mechanisms, the auxin signalling pathway depends on actin organization. The dynamic cortical AFs are necessary for intracellular transport and, thus, interfere with the proper localization of PIN-formed proteins that are essential for auxin export (for review see Nick, 2010). In contrast, bundled actin cables do not contribute. Upon destabilization of the cortical actin meshwork, G-actin is partitioned towards the bundled cables. Therefore, the incidence of bundled cables is correlated with reduced auxin export, but it is not its cause. The cause is the depletion of the dynamic cortical actin meshwork. This conclusion is supported from the finding that direct bundling of actin cables by overexpression of NtVillin 1 does not impair division synchrony (Supplementary Data S3).

In conclusion, abundance and activity of ADF2 could control the dynamic cortical AFs as prerequisite for functional auxin-dependent signalling with respect to synchronized cell division (Campanoni and Nick, 2005; Maisch and Nick, 2007). Dynamics and stability of these cortical AFs must be carefully balanced to keep the actin–auxin oscillator running. Since the non-linear and dynamic activity of ADF2 is expected to involve complexes with other ABPs, titration of complex composition through genetic engineering will be the target of future experiments. In addition, it will be necessary to manipulate the activity of ADF2 by its phosphorylation state and investigate the resulting effects on division synchrony.

## Acknowledgments

This work was supported by the Center for Functional Nanostructures, CFN, Project E1.5, and Sino-German Center for Science Funding, Programme GZ614. We thank A. Görnhardt, O. Huber and S. Purper for technical assistance.

## Appendix A. Supplementary data

Supplementary data associated with this article can be found, in the online version, at <http://dx.doi.org/10.1016/j.jplph.2013.03.002>.

## References

- Allwood EG, Smertenko AP, Hussey PJ. Phosphorylation of plant actin-depolymerising factor by calmodulin-like domain protein kinase. *FEBS Lett* 2001;499:97–100.
- Allwood EG, Anthony RG, Smertenko AP, Reichelt S, Drøbak BK, Doonan JH, et al. Regulation of the pollen-specific actin-depolymerizing factor LIADF1. *Plant Cell* 2002;14:2915–27.
- An G. High efficiency transformation of cultured tobacco cells. *Plant Physiol* 1985;79:568–70.
- Bamberg JR, McGough A, Ono S. Putting a new twist on actin: ADF/cofilins modulate actin dynamics. *Trends Cell Biol* 1999;9:364–70.
- Berghöfer T, Eing C, Flickinger B, Hohenberger P, Wegner LH, Frey W, et al. Nanosecond electric pulses trigger actin responses in plant cells. *Biochem Biophys Res Commun* 2009;387:590–5.
- Berleth T, Sachs T. Plant morphogenesis: long-distance coordination and local patterning. *Curr Opin Plant Biol* 2001;4:57–62.
- Bernstein BW, Bamberg JR. ADF/cofilin: a functional node in cell biology. *Trends Cell Biol* 2010;20:187–95.
- Blanchoin L, Pollard TD. Mechanism of interaction of *Acanthamoeba* actophorin (ADF/cofilin) with actin filaments. *J Biol Chem* 1999;274:15538–46.
- Campanoni P, Blasius B, Nick P. Auxin transport synchronizes the pattern of cell division in a tobacco cell line. *Plant Physiol* 2003;133:1251–60.
- Campanoni P, Nick P. Auxin-dependent cell division and cell elongation: NAA and 2,4-D activate different pathways. *Plant Physiol* 2005;137:939–48.
- Carlier MF, Laurent V, Santolini J, Melki R, Didry D, Xia GX, et al. Actin depolymerizing factor (ADF/cofilin) enhances the rate of filament turnover: implication in actin-based motility. *J Cell Biol* 1997;136:1307–22.
- Chen CY, Wong EI, Vidali L, Estavillo A, Hepler PK, Wu H, et al. The regulation of actin organization by actin-depolymerizing factor in elongating pollen tubes. *Plant Cell* 2002;14:2175–90.
- Chen CY, Cheung AY, Wu HM. Actin-depolymerizing factor mediates Rac/Rop GTPase-regulated pollen tube growth. *Plant Cell* 2003;15:237–49.
- Davies PJ. The plant hormones: their nature, occurrence, and functions. In: Davies PJ, editor. *Plant hormones: biosynthesis, signal transduction, action*. Heidelberg: Springer; 2010. p. 1–15.
- Dhonukshe P, Tanaka H, Goh T, Ebine K, Mänonen AP, Kalika Prasad K, et al. Generation of cell polarity in plants links endocytosis, auxin distribution and cell fate decisions. *Nature* 2008;456:962–7.
- Dong CH, Xia GX, Hong Y, Ramachandran S, Kost B, Chua NH. ADF proteins are involved in the control of flowering and regulate F-actin organization, cell expansion, and organ growth in *Arabidopsis*. *Plant Cell* 2001;13:1333–46.
- Farmer PK, Choi JH. Calcium and phospholipid activation of a recombinant calcium-dependent protein kinase (DCPK1) from carrot (*Daucus carota* L.). *Biochem Biophys Acta* 1999;1434:6–17.
- Friml J. Subcellular trafficking of PIN auxin efflux carriers in auxin transport. *Eur J Cell Biol* 2010;89:231–5.
- Gungabissoon RA, Jiang CJ, Drøbak BK, Maciver SK, Hussey PJ. Interaction of maize actin-depolymerising factor with actin and phosphoinositides and its inhibition of plant phospholipase C. *Plant J* 1998;16:689–96.
- Gungabissoon RA, Khan S, Hussey PJ, Maciver SK. Interaction of elongation factor 1a from *Zea mays* (ZmEF-1a) with F-actin and interplay with the maize actin severing protein, ZmADF3. *Cell Motil Cytoskeleton* 2001;49:104–11.
- Han L, Stope MB, Lopez de Jesus M, Weernink PAO, Urban M, Wieland T, et al. Direct stimulation of receptor-controlled phospholipase D1 by phospho-cofilin. *EMBO J* 2007;26:4189–202.
- Hayden SM, Miller PS, Brauweiler A, Bamberg JR. Analysis of the interactions of actin depolymerizing factor with G- and F-actin. *Biochemistry* 1993;32:9994–10004.
- Hohenberger P, Eing C, Straessner R, Durst S, Frey W, Nick P. Plant actin controls membrane permeability. *Biochim Biophys Acta* 2011;1808:2304–12.
- Holweg C, Süßlin C, Nick P. Capturing *in vivo* dynamics of the actin cytoskeleton stimulated by auxin or light. *Plant Cell Physiol* 2004;45:855–63.
- Hu TX, Yu M, Zhao J. Comparative transcriptional profiling analysis of the two daughter cells from tobacco zygote reveals the transcriptome differences in the apical and basal cells. *BMC Plant Biol* 2010;10:167–83.
- Huang S, Robinson RC, Gao LY, Matsumoto T, Brunet A, Blanchoin L, et al. *Arabidopsis* VILLIN1 generates actin filament cables that are resistant to depolymerization. *Plant Cell* 2005;17:486–501.
- Jiang CJ, Weeds AG, Hussey PJ. The maize actin-depolymerizing factor, ZmADF3, redistributes to the growing tip of elongation root hairs and can be induced to translocate into the nucleus with actin. *Plant J* 1997;12:1035–43.
- Kakimoto T, Shibaoka H. Actin filaments and microtubules in the preprophase band and phragmoplast of tobacco cells. *Protoplasma* 1987;140:151–6.
- Karimi M, Inzé D, Depicker A. Gateway vectors for *Agrobacterium*-mediated plant transformation. *Trends Plant Sci* 2002;7:193–5.
- Ketelaar T, Anthony RG, Hussey PJ. Green fluorescent protein mTalin causes defects in actin organization and cell expansion in *Arabidopsis* and inhibits actin depolymerizing factor's actin depolymerizing activity *in vitro*. *Plant Physiol* 2004;136:3990–8.
- Kleine-Vehn J, Dhonukshe P, Swarup R, Bennett M, Friml J. Subcellular trafficking of the *Arabidopsis* auxin influx carrier AUX1 uses a novel pathway distinct from PIN1. *Plant Cell* 2006;18:3171–81.
- Laňková M, Smith RS, Pešek B, Kubeš M, Zažimalová E, Petrášek J, et al. Auxin influx inhibitors 1-NOA, 2-NOA, and CHPAA interfere with membrane dynamics in tobacco cells. *J Exp Bot* 2010;61:3589–98.
- Lanteri ML, Laxalt AM, Lamattina L. Nitric oxide triggers phosphatidic acid accumulation via phospholipase D during auxin-induced adventitious root formation in cucumber. *Plant Physiol* 2008;147:188–98.
- Lomax TL, Muday GK, Rubery PH. Auxin transport. In: Davies PJ, editor. *Plant hormones: physiology, biochemistry, and molecular biology*. Dordrecht: Kluwer; 1995. p. 509–30.
- Maciver SK, Hussey PJ. The ADF/cofilin family: actin remodeling proteins. *Genome Biol* 2002;3:3007.1–12.

- Maisch J, Nick P. Actin is involved in auxin-dependent patterning. *Plant Physiol* 2007;143:1695–704.
- Maisch J, Fišerová J, Fischer L, Nick P. Actin-related protein 3 labels actin-nucleating sites in tobacco BY-2 cells. *J Exp Bot* 2009;60:603–14.
- Mun JH, Yu HJ, Lee HS, Kwon YM, Lee JS, Lee I, et al. Two closely related cDNA encoding actin-depolymerizing factors of *Petunia* are mainly expressed in vegetative tissues. *Gene* 2000;257:167–76.
- Nagata T, Nemoto Y, Hasezawa S. Tobacco BY-2 cell line as the “Hela” cell in the cell biology of higher plants. *Int Rev Cytol* 1992;132:1–30.
- Nick P. Probing the actin–auxin oscillator. *Plant Signal Behav* 2010;5:4–9.
- Nick P, Han M, An G. Auxin stimulates its own transport by actin reorganization. *Plant Physiol* 2009;151:155–67.
- Nishida E, Iida K, Yonezawa N, Koyasu S, Yahara I, Sakai H. Cofilin is a component of intranuclear and cytoplasmic actin rods induced in cultured cells. *Proc Natl Acad Sci USA* 1987;84:5262–6.
- Normanly J, Slovin JP, Cohen JD. Auxin biosynthesis and metabolism. In: Davies PJ, editor. *Plant hormones: biosynthesis, signal transduction, action*. Heidelberg: Springer; 2010. p. 36–62.
- Olyslaegers G, Verbelen JP. Improved staining of F-actin and colocalization of mitochondria in plant cells. *J Microsc Oxford* 1998;192:73–7.
- Pleskot R, Potocký M, Pejchar P, Linek J, Bezvoda R, Martinec J, et al. Mutual regulation of plant phospholipase D and the actin cytoskeleton. *Plant J* 2010;62:494–507.
- Reinhard D, Mandel T, Kuhlemeier C. Auxin regulates the initiation and radial position of plant lateral organs. *Plant Cell* 2000;12:507–18.
- Sachs T. Integrating cellular and organismic aspects of vascular differentiation. *Plant Cell Physiol* 2000;41:649–56.
- Smertenko A, Franklin-Tong VE. Organisation and regulation of the cytoskeleton in plant programmed cell death. *Cell Death Differ* 2011;18:1263–70.
- Smertenko AP, Jiang CJ, Simmons NJ, Weeds AG, Davies DR, Hussey PJ. Ser6 in the maize actin depolymerizing factor, ZmADF3, is phosphorylated by a calcium stimulated protein kinase and is essential for control of functional activity. *Plant J* 1998;14:187–93.
- Staiger CJ, Poulter NS, Henty JL, Franklin-Tong VE, Blanchoin L. Regulation of actin dynamics by actin-binding proteins in pollen. *J Exp Bot* 2010;61:1969–86.
- Van Troys M, Huyck L, Leyman S, Dhaese S, Vandekerckhove JI, Ampe C. Ins and outs of ADF/cofilin activity and regulation. *Eur J Cell Biol* 2008;87:649–67.
- Waller F, Riemann M, Nick P. A role for actin-driven secretion in auxin-induced growth. *Protoplasma* 2002;219:72–81.
- Wang X. Multiple forms of phospholipase D in plants: the gene family, catalytic and regulatory properties, and cellular functions. *Prog Lipid Res* 2000;39:109–49.
- Zhao H, Hakala M, Lappalainen P. ADF-cofilin binds phosphoinositides in a multivalent manner to act as a PIP<sub>2</sub>-density sensor. *Biophys J* 2010;98:2327–36.